JOURNAL OF GEOPHYSICAL RESEARCH, VOL. 113, A12105, doi:10.1029/2008JA013103, 2008

Interplanetary small- and intermediate-sized magnetic flux ropes during 1995–2005

H. Q. Feng,[1,2] D. J. Wu,[3] C. C. Lin,[4] J. K. Chao,[4] L. C. Lee,[4] and L. H. Lyu[4]

Received 18 February 2008; revised 9 September 2008; accepted 15 October 2008; published 11 December 2008.

[1] We present a comprehensive survey of 125 small- and intermediate-sized interplanetary magnetic flux ropes during solar cycle 23 (1995–2005) using Wind in situ observations near 1 AU. As a result, we found the following: (1) The annual number of small- and intermediate-sized interplanetary magnetic flux ropes is not very sensitive to the solar cycle, but its trend is very similar to that of magnetic clouds (MCs). (2) Average speeds of the individual small- and intermediate-sized interplanetary magnetic flux ropes varied from 289 to 790 km/s with a mean value of 420 ± 86 km/s. Most small- and intermediate-sized interplanetary magnetic flux ropes were found to have a propagation speed similar to typical slow speed solar wind speed, and only a few small- and intermediate-sized interplanetary magnetic flux ropes had speeds comparable to the typically high speed solar wind. (3) Average magnetic field strength for small- and intermediate-sized interplanetary magnetic flux ropes is less than the average magnetic field strengths of MCs, while it is larger than that of background solar wind. (4) The distributions of the axial orientations for small- and intermediate-sized interplanetary magnetic flux ropes are also similar to that of MCs. The results show that small- and intermediate-sized interplanetary magnetic flux ropes and MCs have many similar (or relative) characters. So we suggest that both MCs and small- and intermediate-sized interplanetary magnetic flux ropes originate from solar eruptions.

Citation: Feng, H. Q., D. J. Wu, C. C. Lin, J. K. Chao, L. C. Lee, and L. H. Lyu (2008), Interplanetary small- and intermediate-sized magnetic flux ropes during 1995–2005, *J. Geophys. Res.*, *113*, A12105, doi:10.1029/2008JA013103.

1. Introduction

[2] Magnetic clouds (MCs) are an important subset of interplanetary coronal mass ejections (ICMEs), which are interplanetary manifestations of transient events with large amounts of material ejected from the solar atmosphere [e.g., *Hundhausen*, 1998; *Kahler*, 1988]. A MC was originally defined empirically in terms of in situ spacecraft measurements of magnetic fields and particles in the interplanetary medium at ~1 AU, viz., it has the following necessary properties: (1) the magnetic field direction rotates smoothly through a large angle during an interval of the order of 1 day; (2) the magnetic field strength is higher than average; and (3) low proton temperature compared to the ambient proton temperature [*Burlaga et al.*, 1981, 1990; *Burlaga*, 1995]. MCs, as a kind of large-scale interplanetary magnetic flux rope (IMFR) structure [*Goldstein*, 1983; *Burlaga*, 1988; *Lepping et al.*, 1990; *Farrugia et al.*, 1995; *Burlaga*, 1991], have been investigated and studied by many authors for decades. Some authors found that expansion is a common feature of MCs in the heliosphere, namely the radial size of MCs increases with radial distance from the Sun [e.g., *Burlaga and Behannon*, 1982; *Bothmer and Schwenn*, 1998]. The diameters of MCs are about 0.20 to 0.40 AU near the Earth. Some authors searched for the solar origin of the MCs [e.g., *Smith and Phillips*, 1997; *Bothmer and Schwenn*, 1998; *Leamon et al.*, 2004; *Mandrini et al.*, 2005a] and offered evidence that MCs are the interplanetary manifestations of coronal mass ejections (CME). *Bothmer and Schwenn* [1996] have examined shock events measured by the Hellos 1 spacecraft during the years 1979–1981 for which the associated CME has been directly observed with the coronagraph onboard the P78/1 satellite. They found that 41% of interplanetary manifestations were magnetic clouds. Some other researches focus on the identification of configuration and boundaries of MCs. For example, *Lepping et al.* [1990] identified the cloud axis by minimum variance analysis (MVA) and flux rope fitting (FRF); *Hu and Sonnerup* [2002] obtained the axial orientation on the basis of the Grad-Shafranov equation; *Riley et al.* [2004] identified the cloud configuration with MHD simulation; *Wei et al.* [2003] defined the magnetic cloud boundary as a boundary layer formed through the interaction between the magnetic cloud and the ambient medium; *Feng et al.* [2006] identified the magnetic cloud boundaries in terms of the flux rope configuration of MCs. In addition, geoeffectiveness of

[1] College of Physics and Electronic Information, Luoyang Normal University, Luoyang, China.
[2] State Key Laboratory of Space Weather, Center for Space Science and Applied Research, Chinese Academy of Sciences, Beijing, China.
[3] Purple Mountain Observatory, Chinese Academy of Sciences, Nanjing, China.
[4] Institute of Space Science, National Central University, Jhongli, Taiwan.

0148-0227/08/2008JA013103$09.00

the MCs is another concern [e.g., *Wu and Lepping*, 2002; *Hidalgo*, 2003; *Zhang et al.*, 2004]. *Wu et al.* [2000] studied the interactions between MCs and the magnetosphere and found that the position of the bow shock oscillates quickly in the Sun-Earth line direction during the MCs passage. It is well known that MC is one of the main sources of intense magnetic storms [*Echer and Gonzalez*, 2004].

[3] In addition to large-scale MCs, *Moldwin et al.* [2000] found evidence for the existence of small-scale IMFRs (with duration of ~1 hour) at 1 AU. These small magnetic structures are similar to MCs, and their structures can be fitted with constant-alpha (where $\boldsymbol{J} = \alpha \boldsymbol{B}$), force-free, cylindrically symmetric flux ropes of low plasma beta. *Moldwin et al.* [2000] suggested that these small IMFRs do no originate from the coronal region, instead, the small IMFRs could result from magnetic reconnection at the heliospheric current sheet. The evidence for this argument include as follows: (1) No intermediate-sized events (durations of several hours) have been reported. (2) There is absence of expansion signature within the flux rope. (3) There is a difference in plasma characteristics such as the proton temperature compared to MCs. Recently, *Feng et al.* [2007] provided the size and energy spectrums of IMFRs, which include many small- and intermediate-sized interplanetary magnetic flux ropes. Small- and intermediate-sized interplanetary magnetic flux ropes are defined empirically in terms of magnetic field at ~1 AU in the solar wind. They have the following properties: (1) the magnetic configuration can be described approximately with constant α force-free flux ropes and (2) the durations are not more than 12 hours, and the diameters are usually less than 0.20 AU. Both small- and intermediate-sized interplanetary magnetic flux ropes and MCs are subsets of IMFRs, but they have different sizes. In order to succinctly describe small- and intermediate-sized interplanetary magnetic flux ropes, we will use small magnetic clouds (SMCs) to describe small- and intermediate-sized interplanetary magnetic flux ropes throughout this paper. One of the properties that define MCs is that magnetic field directions rotate smoothly through a large angle during an interval of the order of 1 day, therefore the time durations are usually as long as tens of hours with an average of ~21 hours [*Lepping et al.*, 1990]. For more than three decades, the studies of IMFRs concentrated on MCs with large structure, but there were few studies of SMCs. We expect that the study of SMCs would provide a new aspect to reveal some of the significant physical processes occurring in interplanetary space.

[4] In this paper, we undertake a comprehensive study of a solar cycle of SMC activity, which help demonstrates the general characters. We list 125 SMC events and give their statistical properties, and we also compare their statistical properties with that of MCs.

2. List

[5] For the present study, we use 1 minute averaged plasma and magnetic field data from Wind [*Ogilvie et al.*, 1995]. The main data that we routinely use for the identification of potential SMCs are solar wind magnetic field observations in the GSE Cartesian coordinate system, where x is along the Earth-Sun line and points to the Sun, y points to the dusk in the ecliptic plane (opposing planetary motion), and z points to the ecliptic north pole. The reason is that smooth and slow rotation of the magnetic field is the essential character of IMFRs. Here we identify a SMC through the following steps: (1) The candidate SMC was selected by identifying the rotation of magnetic field direction and enhanced magnetic field strength (compared to the ambient medium) by eye; The rotations include bipolar signature, increasing slowly from minimum to maximum or/and decreasing maximum to minimum. For the potential events, y and z components always have obvious rotations; sometimes, the x component also has a rotation. (2) Then we use the geometric parameter of the flux rope to identify the possible events, namely we defined it as the magnetic field variation which can be fitted to the cylindrical constant-alpha force-free field. When the difference between the model geometry and the observation data was larger than a criterion value ($\sqrt{\chi^2} = 0.3$), the case was not considered as a flux rope. The deviation can be expressed by the minimum chi-square χ^2 (see equation (2)). Last we identified 125 SMCs, which are listed in Table 1. However, we do not rule out the possibility that we missed some events due to data gaps or noise.

[6] Using the model first established by *Goldstein* [1983], we consider the constant alpha force-free field configuration an approximation for the SMCs, i.e., the SMCs can be described with *Lundquist* [1950] solution:

$$\begin{cases} B_R = 0 & \text{(Radial component)} \\ B_T = HB_0 J_1(\alpha R) & \text{(Tangential component)} \\ B_A = B_0 J_0(\alpha R) & \text{(Axial component)} \end{cases} \quad (1)$$

where J_n is the n-order Bessel function, $H = \pm 1$ denotes the right and left handedness of the field twist, respectively, B_0 is the field intensity at the axis of the rope, and R is the radial distance from the axis. For a magnetic flux rope, if the axial vector ($\boldsymbol{m}$) and the spacecraft trajectory (denoted by unit vector $\boldsymbol{s}$) are given, one can set up the so-called rope coordinate system ($\boldsymbol{l}$, $\boldsymbol{m}$, $\boldsymbol{n}$): $\boldsymbol{m}$ axis is along the rope's axis; the cross product $\boldsymbol{m} \times \boldsymbol{s}$ is the $\boldsymbol{n}$ axis; the cyclic triad $\boldsymbol{l}$, $\boldsymbol{m}$, $\boldsymbol{n}$ forms a right-hand set. The flux rope configuration can be displayed in the rope coordinate system by measured magnetic fields. Notice that the profiles of all the three magnetic components depend on only d_0/R_0, where d_0 is the minimum distance between the spacecraft trajectory and the cloud axis, and R_0 is the rope's radius. If the spacecraft crosses near (or through) the axis, the l component is zero at the center and slowly increases to the maximum at the boundary, the m component is zero at the boundary and slowly increases to the maximum at the center, and the n component approximately keep a small value (or zero). If the spacecraft trajectory considerably departs from the axis, the profiles of the l and m component will not change, but the n component is a smaller value (not zero) at the boundary and slowly increases to the maximum at the center [*Feng et al.*, 2007]. *Lepping et al.* [1990, 2003] and *Moldwin et al.* [2000] fitted MCs and small-scale IMFRs respectively using the method of *Lepping et al.* [1990]. We also fit SMCs here using this method, i.e., the least squares fit. Because of the

Table 1. Fitting Parameters and Average Values of SMCs, 1995–2005 (Observed Data From Wind)

No.[a]	Start[b]	End[c]	Δt[d]	ϕ_A[e]	θ_A[f]	χ[g]	d_0/R_0[h]	2 R_0[i]	B_0[j]	H[k]	V[l]	N[m]	B[n]
001	199503070400	199503070803	4.05	263	−50	0.2075	0.83	0.0712	12.1	−1	414	4.6	7.2
002	199503072317	199503080043	1.43	285	−11	0.1222	0.66	0.0183	10.8	1	445	5.3	7.1
003	199503241131	199503241615	4.73	327	−68	0.2131	0.31	0.0373	10.8	−1	328	16.1	8.2
004	199505020438	199505020534	0.96	228	23	0.2231	0.73	0.0123	19.3	1	472	16.1	12.9
005	199505131050	199505131625	5.58	176	19	0.1744	0.95	0.0469	17.7	−1	327	13.4	10.1
006	199505291347	199505291628	2.68	146	26	0.2471	0.63	0.0232	15.9	−1	416	19.9	11.6
007	199506172143	199506180437	6.90	334	23	0.2037	0.03	0.0307	5.8	1	350	16.8	10.5
008	199506180646	199506181529	8.72	273	−13	0.2369	0.13	0.0946	11.5	1	333	14.8	5.5
009	199508110441	199508110556	1.25	298	33	0.1466	0.85	0.0255	9.9	−1	479	5.7	5.8
010	199508151419	199508151720	3.02	277	−66	0.1966	0.66	0.0552	9.0	−1	568	2.5	5.8
011	199508172056	199508180158	5.03	205	−78	0.1979	0.70	0.1059	13.7	−1	404	13.1	8.9
012	199509201300	199509201401	1.02	217	16	0.1640	0.00	0.0059	8.6	1	374	30.7	6.6
013	199509210255	199509210454	1.98	216	13	0.1317	0.62	0.0151	9.2	1	396	18.4	5.9
014	199509271355	199509272102	7.12	327	48	0.2746	0.51	0.0667	16.9	−1	403	15.0	13.4
015	199602030238	199602030405	1.45	282	72	0.0651	0.97	0.0714	10.4	−1	487	3.6	4.9
016	199602101741	199602102208	4.45	41	−74	0.2025	0.90	0.1025	16.3	−1	424	9.1	9.9
017	199603031338	199603031451	1.22	319	−21	0.1240	0.85	0.0150	11.0	1	367	10.8	6.5
018	199603080028	199603080636	6.13	78	−44	0.1571	0.01	0.0507	6.3	1	346	16.5	6.0
019	199603081947	199603090231	6.73	100	−11	0.2890	0.07	0.0515	5.8	−1	320	9.8	5.5
020	199603090919	199603091350	4.52	128	32	0.2038	0.53	0.0379	4.8	−1	338	20.5	6.4
021	199603130941	199603131021	0.67	327	69	0.0928	0.32	0.0096	13.6	−1	570	5.0	9.6
022	199605020543	199605020647	1.07	318	7	0.1826	0.05	0.0137	7.1	−1	389	15.8	4.9
023	199605170101	199605170950	8.82	286	−1	0.2061	0.01	0.0863	7.9	−1	422	6.1	7.2
024	199607201843	199607201958	1.25	330	−26	0.1384	0.60	0.0108	9.4	−1	449	8.1	6.5
025	199609281302	199609281405	1.05	265	15	0.1556	0.44	0.0130	7.3	−1	465	3.7	5.0
026	199703180720	199703180842	1.37	325	−19	0.0923	0.88	0.0164	7.3	1	370	9.8	3.8
027	199704261041	199704261144	1.05	314	−27	0.1195	0.64	0.0092	3.3	1	346	10.2	2.2
028	199705090457	199705090853	3.93	221	−39	0.2866	0.52	0.0277	7.3	1	306	11.8	5.6
029	199705111141	199705111401	2.33	335	−31	0.2601	0.05	0.0116	5.6	1	326	9.9	5.0
030	199705120524	199705120742	2.30	267	41	0.2101	0.52	0.0197	5.2	1	300	11.9	4.2
031	199705160615	199705161324	7.15	319	15	0.1625	0.49	0.0665	10.9	−1	490	3.5	7.9
032	199705230620	199705231218	5.96	145	9	0.2403	0.00	0.0258	2.9	1	303	7.4	2.3
033	199705240222	199705240730	5.13	337	20	0.2257	0.01	0.0366	6.0	−1	318	15.4	5.2
034	199705251915	199705260244	7.48	317	−61	0.1496	0.00	0.0508	8.4	−1	311	10.1	5.6
035	199706190531	199706191557	10.43	231	−52	0.1925	0.01	0.0830	9.4	1	358	8.0	8.3
036	199707200842	199707201022	1.67	273	−37	0.1635	0.66	0.0265	10.0	−1	492	3.8	6.4
037	199707201049	199707201210	1.35	323	−25	0.2648	0.01	0.0107	7.3	−1	475	2.9	6.2
038	199707232054	199707232214	1.33	310	20	0.1459	0.61	0.0118	7.9	−1	363	11.6	5.1
039	199707240700	199707240727	0.45	211	13	0.2463	0.81	0.0039	15.4	1	394	16.4	9.9
040	199707240731	199707240902	1.52	209	−12	0.1769	0.56	0.0067	13.4	1	405	14.0	9.8
041	199709031324	199709032038	7.23	281	−6	0.1227	0.37	0.0743	17.0	1	403	13.7	13.8
042	199709271514	199709271654	1.67	315	44	0.2624	0.25	0.0137	10.8	1	395	12.0	8.9
043	199801081544	199801082107	5.38	328	41	0.1780	0.41	0.0976	20.3	1	361	12.7	9.8
044	199801251254	199801251857	6.05	114	−51	0.1872	0.13	0.0577	7.6	−1	404	9.6	6.2
045	199802182111	199802190756	10.75	25	−39	0.2188	0.63	0.0972	15.6	−1	409	2.1	10.4
046	199802270540	199802270828	2.80	219	−9	0.1584	0.49	0.0159	9.5	1	316	10.1	6.3
047	199803061429	199803062204	7.58	318	−41	0.1827	0.00	0.0506	5.9	1	333	11.6	5.3
048	199803251328	199803251618	2.83	123	11	0.1721	0.28	0.0242	13.1	1	402	8.9	9.6
049	199803282247	199803290211	3.40	248	3	0.2262	0.56	0.0430	12.8	1	466	4.3	8.8
050	199805152147	199805160154	4.12	359	−61	0.2694	0.00	0.0328	13.9	−1	381	10.8	12.9
051	199806021030	199806021556	5.43	70	15	0.0498	0.10	0.045	11.8	−1	400	7.2	10.9
052	199806260004	199806260749	7.75	330	20	0.2002	0.42	0.0594	16.4	−1	470	9.7	12.7
053	199811080442	199811081434	9.87	221	−30	0.1929	0.51	0.1259	41.3	−1	515	15.9	21.7
054	199902170713	199902170958	2.75	206	17	0.1471	0.62	0.0173	21.3	−1	622	8.9	9.2
055	199905240936	199905241028	0.87	214	−34	0.1838	0.24	0.0132	8.3	−1	447	12.4	6.7
056	199909212026	199909220546	9.33	270	12	0.1588	0.49	0.0923	15.1	−1	357	12.8	11.6
057	200002121340	200002130032	10.87	201	−51	0.1387	0.55	0.0688	13.9	−1	546	6.4	11.4
058	200004181521	200004181743	2.37	276	−22	0.1849	0.57	0.0285	6.3	1	405	5.4	4.8
059	200004210709	200004210932	2.38	252	40	0.1146	0.73	0.0401	9.3	1	488	3.2	6.3
060	200004271522	200004271828	3.10	200	78	0.1519	0.14	0.0299	8.0	1	402	9.7	7.0
061	200004271900	200004272314	4.23	224	57	0.2449	0.00	0.0374	11.0	−1	395	14.2	10.2
062	200005050404	200005050609	2.08	223	−40	0.1042	0.89	0.0376	10.7	−1	411	4.3	5.5
063	200007260414	200007260832	4.30	221	−25	0.1927	0.59	0.0355	14.7	−1	377	8.8	11.0
064	200008230923	200008231201	2.63	316	57	0.0815	0.80	0.0299	18.6	−1	304	10.7	10.7
065	200009190906	200009191309	4.05	319	−51	0.2375	0.15	0.0576	10.1	−1	661	6.3	8.2
066	200012231555	200012232137	5.70	45	5	0.2946	0.59	0.0360	9.1	1	300	11.8	7.1
067	200101082059	200101082352	2.88	80	28	0.2115	0.00	0.0279	7.8	1	402	9.8	7.5
068	200101090044	200101090224	1.67	296	6	0.2594	0.40	0.0277	7.0	−1	411	9.2	6.6
069	200101090242	200101090320	0.63	218	−47	0.1307	0.01	0.0055	8.7	1	404	8.4	6.7
070	200101090929	200101091417	4.80	204	38	0.2075	0.86	0.0658	7.1	1	409	3.5	4.5
071	200104081553	200104081958	4.83	220	52	0.1335	0.94	0.2083	28.0	1	789	6.8	16.3
072	200104120750	200104121754	10.67	205	23	0.1474	0.78	0.1364	21.8	1	637	1.6	15.0
073	200108252007	200108260003	3.93	231	3	0.1999	0.92	0.0794	20.0	1	419	17.9	11.2

Table 1. (continued)

No.[a]	Start[b]	End[c]	Δt[d]	ϕ_A[e]	θ_A[f]	χ[g]	d_0/R_0[h]	2 R_0[i]	B_0[j]	H[k]	V[l]	N[m]	B[n]
074	200109261024	200109261715	6.85	300	45	0.1578	0.87	0.1833	23.0	1	590	5.7	12.2
075	200110051801	200110052144	3.73	195	−24	0.1089	0.78	0.0265	6.4	1	392	9.5	4.6
076	200110150833	200110150912	0.66	12	4	0.1876	0.68	0.0022	5.4	−1	458	5.0	4.5
077	200112051518	200112051730	3.21	334	−41	0.2594	0.01	0.0243	9.5	1	429	5.2	8.5
078	200112150914	200112150955	0.69	169	−2	0.1449	0.87	0.0022	15.8	1	329	25.9	11.0
079	200201192108	200201192145	0.61	252	−55	0.1881	0.90	0.0140	10.2	1	423	26.9	8.0
080	200201250840	200201251149	3.15	50	24	0.1523	0.71	0.0285	12.0	−1	330	16.7	8.3
081	200202182145	200202190249	5.06	292	−47	0.2406	0.46	0.0464	12.1	1	350	22.4	9.6
082	200202282100	200203010259	6.00	194	15	0.2466	0.82	0.0340	21.0	1	387	17.3	13.0
083	200203070135	200203070221	0.77	177	1	0.1916	0.79	0.0011	7.4	1	624	2.9	4.9
084	200203171932	200203172116	1.74	335	10	0.1741	0.77	0.0086	9.6	−1	289	11.5	5.8
085	200203270250	200203270408	1.31	42	−1	0.2280	0.02	0.0104	4.0	1	494	3.0	3.3
086	200204070948	200204071140	1.89	175	3	0.2005	0.61	0.0024	10.0	1	411	5.2	7.9
087	200205101732	200205101956	1.39	360	39	0.2818	0.01	0.0085	10.1	−1	403	22.1	10.0
088	200206021828	200206022141	3.20	76	−5	0.1723	0.44	0.0339	11.7	−1	409	8.1	9.5
089	200206072030	200206072324	2.89	230	−21	0.2296	0.73	0.0238	7.5	1	292	9.1	5.1
090	200206190401	200206190543	1.67	100	12	0.1970	0.01	0.0167	14.4	1	420	20.8	12.2
091	200207011302	200207011554	2.88	55	19	0.1622	0.84	0.0459	13.4	1	434	7.3	8.2
092	200207050251	200207050352	1.03	163	−3	0.2631	0.00	0.0026	6.9	1	353	24.1	5.0
093	200207120410	200207120905	4.90	166	−5	0.2234	0.59	0.0156	16.7	1	418	15.6	12.7
094	200208191249	200208191405	1.29	232	24	0.1179	0.81	0.0229	13.9	1	522	12.4	8.1
095	200209191514	200209191558	0.73	265	−5	0.2804	0.10	0.0088	6.7	−1	502	8.0	7.1
096	200209241941	200209242139	1.97	199	−12	0.0917	0.72	0.0095	12.5	−1	371	2.0	8.3
097	200210030956	200210031732	7.60	174	1	0.1221	0.86	0.0174	19.5	1	457	8.3	11.3
098	200210310221	200210310351	1.50	345	−5	0.2795	0.47	0.0050	9.3	−1	448	5.0	8.4
099	200211102307	200211110058	1.56	32	17	0.1300	0.88	0.1560	26.2	−1	408	8.6	8.2
100	200211112007	200211112105	0.97	309	−24	0.1565	0.18	0.0127	9.6	1	655	4.8	6.9
101	200211141450	200211141628	1.67	51	−7	0.2170	0.49	0.0162	9.8	−1	453	7.8	7.8
102	200211240703	200211240832	1.48	352	18	0.2049	0.01	0.0054	7.2	−1	454	5.0	7.0
103	200212222104	200212230038	3.58	175	−18	0.1418	0.00	0.0136	19.5	1	494	18.3	14.9
104	200212261828	200212261923	0.91	275	23	0.2581	0.01	0.0102	14.3	−1	468	15.1	11.3
105	200301121429	200301121719	2.86	101	−8	0.0648	0.88	0.0514	15.6	−1	362	4.7	9.0
106	200301141310	200301141540	2.51	60	48	0.1425	0.64	0.0286	12.9	−1	387	7.9	8.8
107	200301170922	200301171332	4.18	237	−13	0.1449	0.66	0.0369	12.3	1	327	18.8	8.3
108	200302060600	200302060726	1.43	241	−39	0.2476	0.67	0.0198	12.3	−1	528	15.2	7.7
109	200302110525	200302110741	2.26	215	5	0.1523	0.65	0.0176	11.0	1	420	8.6	6.9
110	200304291648	200304291852	2.08	42	−29	0.1000	0.89	0.0452	6.2	−1	544	3.2	11.9
111	200307221011	200307221138	1.46	292	7	0.1204	0.71	0.0201	8.5	1	435	3.1	6.2
112	200308050824	200308051021	1.96	354	42	0.1375	0.76	0.0224	13.0	−1	457	8.4	8.7
113	200309292209	200309300124	3.27	346	−68	0.2254	0.47	0.0247	5.8	1	297	13.5	4.6
114	200403050241	200403050412	1.54	334	29	0.0762	0.77	0.0168	8.1	1	471	4.9	5.4
115	200404080357	200404080611	2.24	76	−7	0.1411	0.63	0.0310	4.8	−1	460	4.7	6.4
116	200406090651	200406090911	2.35	291	9	0.0970	0.02	0.0237	8.0	1	444	4.4	7.2
117	200408022338	200408030100	1.35	93	41	0.1755	0.68	0.0176	7.2	−1	398	5.7	4.4
118	200410081618	200410082003	3.76	97	15	0.1470	0.51	0.0355	12.3	−1	342	11.	9.1
119	200410110232	200410110602	3.51	334	−8	0.2877	0.01	0.0156	8.3	−1	404	5.6	7.3
120	200502200009	200502200441	4.54	53	54	0.2119	0.03	0.0515	10.2	−1	506	4.0	9.0
121	200503050729	200503050924	1.92	171	−44	0.1772	0.43	0.0145	7.6	1	404	15.1	6.3
122	200504181802	200504181945	1.72	73	−7	0.2328	0.59	0.0179	5.6	−1	365	5.9	4.1
123	200507310048	200507310222	1.57	92	83	0.1628	0.49	0.0205	8.0	−1	473	5.6	6.3
124	200510162014	200510162147	1.54	163	13	0.2805	0.55	0.0058	9.2	1	363	6.8	7.7
125	200511110011	200511110058	0.78	160	16	0.2135	0.74	0.0042	4.9	1	351	18.3	4.9

[a]The code number of the SMC.
[b]The beginning of the SMC (UT).
[c]The end of the SMC (UT).
[d]The Δt is duration of the event (h).
[e]The longitude of the rope's axis measured counterclockwise in an ecliptic coordinate system, where $\phi_A = 0°$ represents toward the Sun.
[f]The latitude of the rope's axis in an ecliptic coordinate system.
[g]The square root of the chi-square value.
[h]The ratio of the closest approach distance to the Radius.
[i]The diameter of the SMC (AU).
[j]The rope's axial magnetic field strength (nT).
[k]The sign of the handedness of the rope.
[l]The average speed for the SMC (km/s).
[m]The average proton density for the SMC (cm^{-3}).
[n]The average magnetic field magnitude for the SMC (nT).

great value of the x-GSE component of the solar wind velocity, the path of the spacecraft relative to the flux rope is almost parallel to the x-GSE direction [*Hidalgo and Cid*, 2002]. Combining the axial direction (i.e., by θ_A, ϕ_A the latitude and longitude of the axis, given with respect to the ecliptic plane), one can set up the rope coordinate system. Then the observed field (unit normalized) in the GSE coordinate system is transformed into the rope coordinates

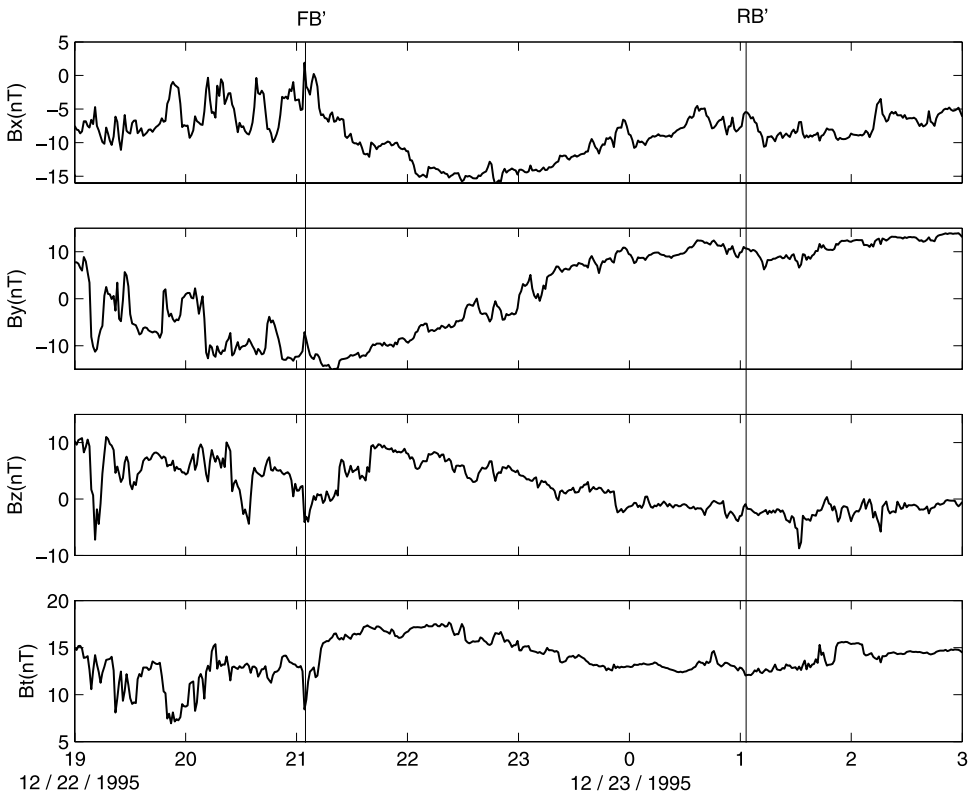

Figure 1. Interplanetary magnetic field data measured by the Wind spacecraft in the GSE coordinate system. FB′ and RB′ are the estimated front and rear boundaries, respectively.

that can be found through a series of iterations to finally reach the minimum chi-square:

$$\chi^2 = \sum_{i=1}^{N} \left[\left(B_{xc}^O - B_{xc}^M\right)^2 + \left(B_{yc}^O - B_{yc}^M\right)^2 + \left(B_{zv}^O - B_{zc}^M\right)^2 \right] \Big/ 3N, \tag{2}$$

where N is the number of field vectors (hour averages were used to fit MCs by *Lepping et al.* [1990] and minute averages were used to fit small-scale flux ropes [*Moldwin et al.*, 2000]; here we take $N = 25$, i.e., 25 share-averages, the duration of the SMC was divided into 25 equal shares), and the subscript c refers to the cloud coordinate, superscripts M and O refer to the model and observed fields. The least squares analysis can provid e axial orientation (θ_A, ϕ_A) and d_0/R_0. On basis of the fitting axial orientation (θ_A, ϕ_A), we can set up the final rope coordinate system. In the final rope coordinate system, a single least squares fit to B_0 (the field strength on the axis of the rope) is done. Namely the observed field (without normalizing) transformed into the final rope coordinates that can be found through variance B_0 to reach the minimum chi-square (similar to equation (2)). The more detailed descriptions can be found in the work of *Lepping et al.* [1990, 2003]. The fitting parameters of all the 125 SMCs are listed in Table 1.

[7] The identification of boundaries of IMFRs has been an important problem in the investigations related to IMFRs, however, the boundaries of flux ropes are not always evident. We confirm the boundaries through the following steps: At first, the boundaries can be estimated using the rotation of magnetic field and enhanced magnetic field strength. Second, the orientation of the axis is confirmed using flux rope fitting, and the final rope coordinate system can be established by the obtained axial orientation. Last the interplanetary magnetic field data, which are measured in GSE coordinate and are converted into the final rope coordinate system. In the final rope coordinate system, the global structure of the flux rope can be displayed clearly and the boundaries can be easily identified. It is necessary to point out that in using this method a certain degree of subjectivity seems unavoidable. However, the estimated boundaries should not depart significantly from the actual rope boundaries. In the following paragraph, we will introduce an IMFR as example. The detailed description of this method is in the work of *Feng et al.* [2006]. Given the boundaries of SMCs, one can calculate the mean speed V, density N, magnetic field strength B in each of the SMCs. The identified front and rear boundaries, duration, mean density and magnetic field strength are also listed in Table 1.

[8] The data of the interplanetary magnetic field of the 22–23 December 2002 SMC event are shown in Figure 1 (in the GSE coordinates). From top to bottom, the panels show the x, y, z components of the magnetic field (Bx, By, Bz), and the magnitude of the total magnetic field (Bt), respectively. As seen in Figure 1, the total magnetic field magnitude begins to enhance at 21:04 UT on December 22 (denoted by the vertical solid line FB1), in which the smooth field rotations seem to begin, too. In addition, the total magnetic field magnitude decreases to a minimum at 01:03 UT on December 23 (denoted by RB1). So we take FB1 and RB1 as the potential front and rear boundaries to fit the potential SMC event. The fitting results display that

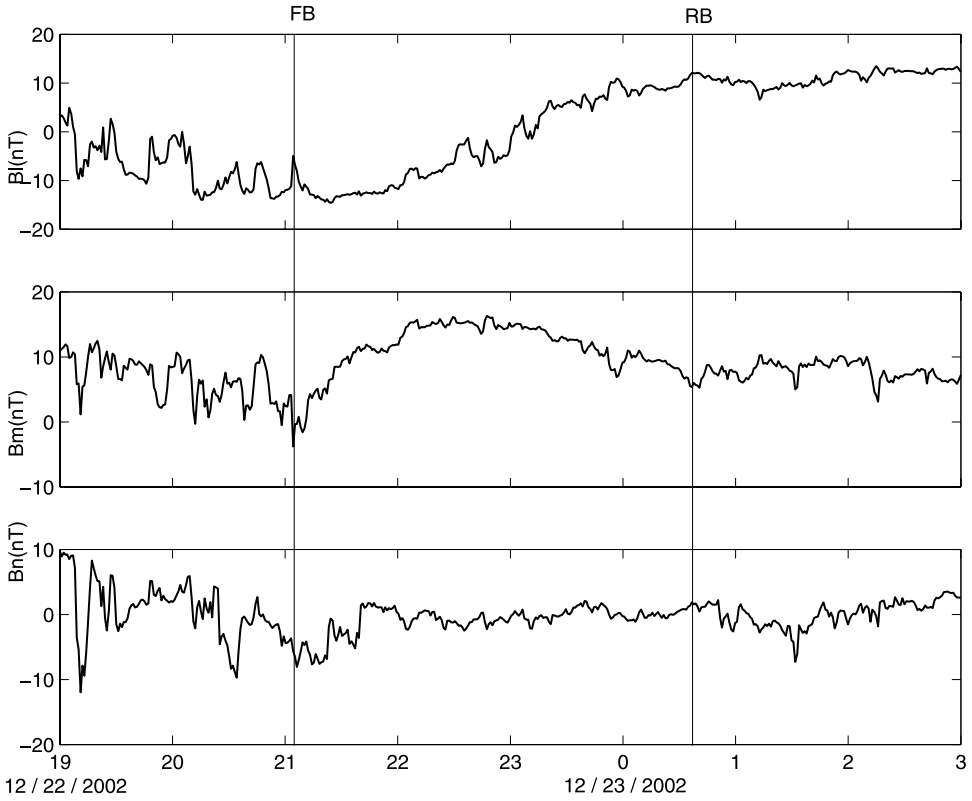

Figure 2. Variation of magnetic field components in the rope natural system, coordinate system associated with primal fitting axial direction ($\theta_A = -16°$, $\phi_A = 173°$). FB and RB are identified front and rear boundaries, respectively.

the minimum chi-square $\chi^2 = 0.0213$, $d_0/R_0 = 0.04$, and the axial direction is ($\theta_A = -16°$, $\phi_A = 173°$). On the basis of the fitting axial direction, the final rope coordinate system was established, and the interplanetary magnetic field data, which are measured in GSE coordinate and are converted into the final rope coordinate system (Figure 2). From Figure 2 one can find that there is an apparent flux tube profile between FB and RB. Around RB, the *m* component slowly increases to the maximum at RB, and the *l* component decreases to the minimum. So it is proper to identify FB and RB as the rope's boundaries.

[9] Once the boundaries were confirmed, we can fit the observed flux rope again. The new fitting results are that the minimum chi-square $\chi^2 = 0.0201$, $d_0/R_0 = 0.00$, and the axial direction is ($\theta_A = -18°$, $\phi_A = 175°$). The transformed magnetic fields are shown by solid curves in Figure 3. The dashed curves are the least squares fitting results of the constant alpha flux rope model based on the observed data. It can be found that the model fits well to the observed data except that the *Bn* component is only slightly mismatched. In addition, we can find that the fitting results are at close range with different selected boundaries. So the veracity of initially estimated boundaries is not important, one can select different potential boundaries to fit in an iterative manner.

3. Statistical Properties

3.1. Occurrence Rates

[10] The annual numbers of SMCs from 1995 to 2005 are given in Table 2. In Figure 4, we also show the occurrence rates of SMCs and MCs. The MCs have been identified using Wind data in the literature [*Feng et al.*, 2007; *Wu et al.*, 2007] and published on the Website of Wind MFI team http://lepmfi.gsfc.nasa.gov/mfi/mag_cloud_S1.html. According to general expectation, the yearly number of MCs should increase from solar minimum to maximum. However, the statistical results reveal that the occurrence rates did not continuously increase from solar minimum to maximum. However, from Figure 4, one can easily find that the trends of two sets of curves are very similar except for the maximum number of SMCs in 2002. This implies that both the MCs and SMCs originate from solar eruptions. And as for the high occurrence rate of SMCs in 2002, we cannot find the direct origin from the data of both solar and space spacecraft. The high occurrence rate of SMCs in 2002 may result from the specifically eruption conditions in the solar corona, where the SMCs are easy to produce. From Figure 4 we can see that not only for MCs, but also for SMCs there is a temporary clear decrease in the occurrence rate in 1999, and then the rate increases again in the following year. Actually the same phenomenon also occurs for ICME, and the unusually low occurrence rate in 1999 was first noted by *Cane et al.* [2000]. Then *Cane and Richardson* [2003] gave an explanation that the decline is associated with an increase of corotating high speed streams from low-latitude coronal holes and the restructuring of the near ecliptic solar wind in 1999. However, *Wu et al.* [2006] showed that the number of observed CMEs does not decrease in 1999, instead, it increases during the years 1996 to 2002. *Gopalswamy et al.* [2003] explains that the drought of ICMEs/MCs at and around 1999 is due to

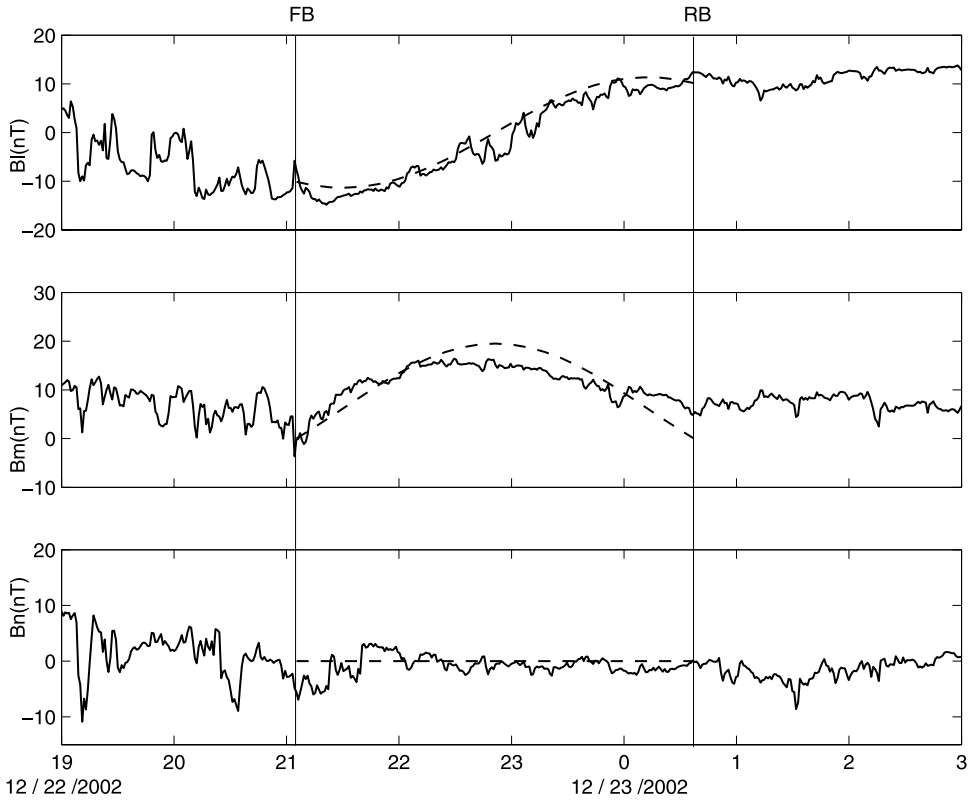

Figure 3. Variation of magnetic field components in the rope natural system coordinate system associated with fitting axial direction ($\theta_A = -18°$, $\phi_A = 175°$) and the flux rope fitting curves (dashed curves). FB and RB are identified front and rear boundaries, respectively.

a migration of the sources of CME on the solar surface. The sources move to higher latitudes such that the associated ejecta will not reach the Earth. In general, the number of the CMEs observed at low solar latitude has a good correlation with the number of ICMEs/MCs observed at 1 AU. Therefore the decline of occurrence rates of SMCs in 1999 may be related to the solar activity. In addition, from Figure 4 we can find that the number of SMCs was much larger than that of MCs as well.

3.2. Average Properties of SMCs

[11] Table 2 lists the average properties of the SMCs and their variation as a function of years. Average speeds of the individual SMCs varied from 289 to 790 km s^{-1} with a mean value of 420 ± 86 km s^{-1}. The annual average speeds are higher around solar maximum and lower around solar minimum. However, there is no continuous increase from solar minimum to maximum. Figure 5 shows a histogram in 50 km s^{-1} bins for the average speeds V (derived from the protons only). Most SMCs were found to have a propagation speed similar to that of typically slow speed (300–500 km s^{-1}) solar wind. Only a few SMCs had speeds comparable to the typically high (700–800 km s^{-1}) speed solar wind. The peak of the speed distribution in Figure 5 lies in the range 400–450 km s^{-1}. The distribution for average speed of SMCs is similar to that of MCs, which were obtained using the Helios data for the period 1974–1981 by *Bothmer and Schwenn* [1998]. However, unlike the MCs that have decreasing velocity profiles, the velocity profiles in SMCs are always flat (i.e., no expansion) and consistent with the immediately surrounding solar wind. For a few events, there are some fluctuations in the velocity curves.

[12] The averaged magnetic field strength of the SMCs varies from 2.2 to 21.8 nT with a mean value of 8.1 ± 3.1 nT. In contrast with the averaged magnetic field strength (12.9 nT) of the MCs, which is derived from the Wind observations for the years 1995–2003 [*Wu and Lepping*, 2007], the averaged magnetic field strength of the SMCs is small. However, the averaged magnetic field strength of the SMCs is larger than that of the averaged solar wind (6.1 nT), which is derived from Wind observed solar wind data for the years 1996–2003 [*Gopalswamy*, 2006]. An IMFR usually has an enhanced magnetic field strength, and an MC, as a larger-scale flux rope, usually has a higher magnetic field strength. So it is not surprising that the

Table 2. Average Properties of SMCs

Year	No.	Average V (km/s)	Average N (cm^{-3})	Average B (nT)
1995	14	408 ± 67	13.7 ± 7.4	8.6 ± 2.7
1996	11	416 ± 74	9.9 ± 5.6	6.6 ± 1.7
1997	17	374 ± 64	10.1 ± 4.0	6.5 ± 3.0
1998	11	405 ± 60	9.4 ± 3.8	10.5 ± 4.5
1999	3	475 ± 134	11.4 ± 2.1	9.2 ± 2.4
2000	10	429 ± 109	8.0 ± 3.4	8.3 ± 2.4
2001	12	472 ± 131	9.0 ± 6.7	9.1 ± 4.1
2002	26	433 ± 85	11.9 ± 7.3	8.6 ± 2.8
2003	9	417 ± 84	9.3 ± 5.5	8.1 ± 2.0
2004	6	420 ± 48	6.1 ± 2.6	6.7 ± 1.7
2005	6	410 ± 64	9.8 ± 5.9	6.4 ± 1.7
All	124	420 ± 86	10.3 ± 5.8	8.1 ± 3.1

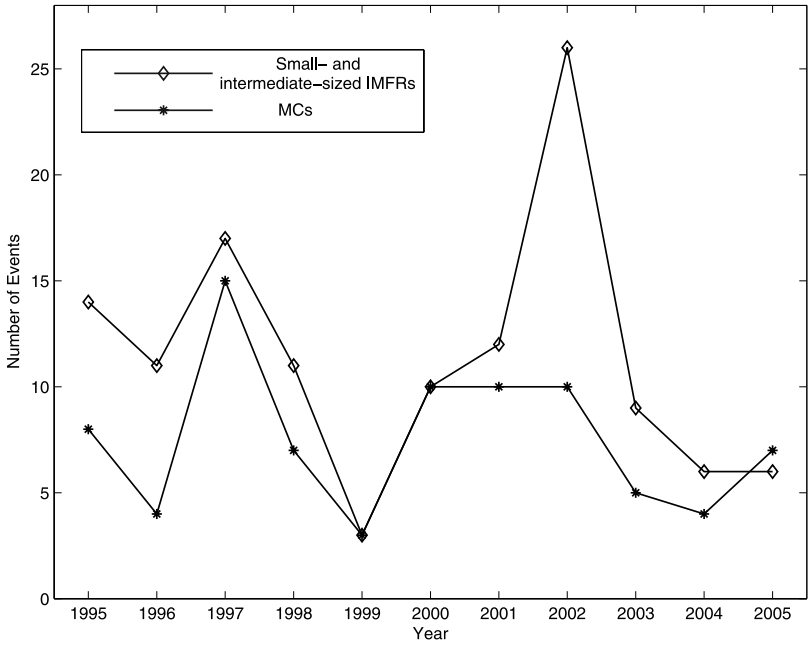

Figure 4. Comparison of the year average number of SMCs and MCs as observed by wind over solar cycle 23.

averaged magnetic field strength of the SMCs is less than that for the MCs, but larger than that of the background solar wind. The distribution of the averaged magnetic field strength for SMCs is also shown in Figure 6. It can be seen that for most cases the averaged magnetic field strength is between 4 to 12 nT, while there are only 18 SMCs with an averaged magnetic field strength out of the interval.

[13] The average densities of SMCs varied from 1.7 to 30.7 cm^{-3} with a mean value of 10.3 ± 5.8 cm^{-3}, which is slightly more than the average density for MCs (9.4 cm^{-3}) [*Wu and Lepping*, 2007]. The proton density in MCs is consistently lower than the ambient solar wind, but the density changes very little across SMCs. We suggest that SMCs also have lower density originally. However, the magnetic field is weaker inside SMCs, and the ion gyroradius is larger. So the densities in SMCs easily diffuse and mix with the ambient solar wind during their propagation in the solar wind.

3.3. Diameter Distribution of SMCs

[14] On the basis of the model fitting, the ninth column of Table 1 gives the calculated diameters of these SMCs. The

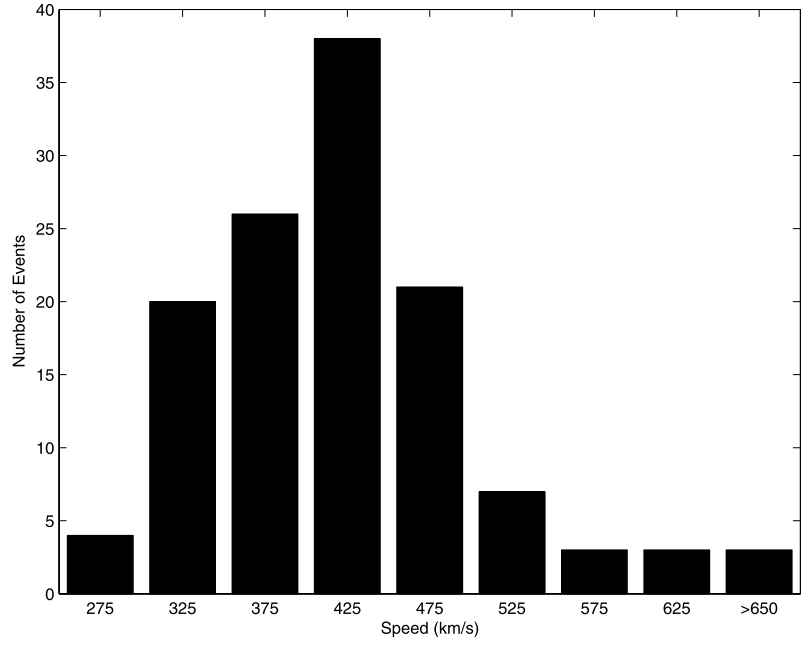

Figure 5. The distributions for the average proton speeds of SMCs in bins of km s^{-1}.

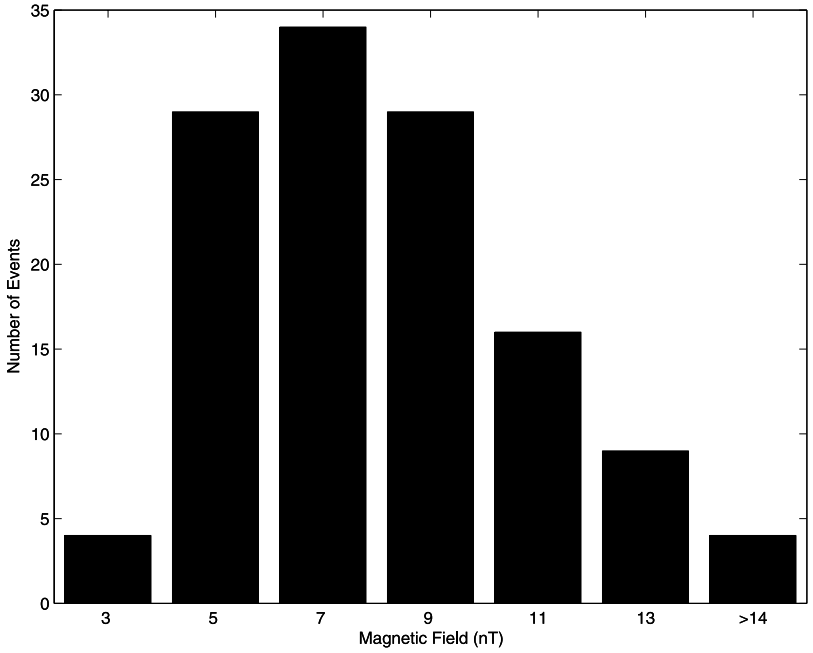

Figure 6. The distribution for the average magnetic field strength of SMCs.

distribution of the diameters for the SMCs is shown in Figure 7. One can find that most diameters of SMCs are much smaller than that of MCs (0.2–0.4 AU) [*Burlaga*, 1988]. The peak of the distribution lies from 0.01 to 0.02 AU. Although the number of flux ropes for 0–0.01 AU is smaller than that for 0.01–0.02 AU, the rough trend of distribution shows that the occurrence rate of SMCs decreases with the diameter. There are Alfvénic fluctuations [*Mariani and Neubauer*, 1990], shocks and other small-scale structures associated with large variations in the magnetic field direction [*Marsch*, 1991] in the solar wind. In addition, Alfvén waves and other small-scale fluctuations are likely to interfere with the identifications of small-scale flux ropes. So the number of identified flux ropes for 0.00–0.01 AU is smaller.

3.4. Axial Orientation of SMCs

[15] In this section we discuss the axial orientation for the 125 SMCs. Both SMCs and MCs are magnetic flux ropes, if they all come from the CME eruptions, they may have similar statistical results. The frequency distribution of the fitted longitude orientations is shown in Figure 8. For ease of comparison with other previous statistical results of MCs, all longitudes greater than 180° had 180° subtracted to force

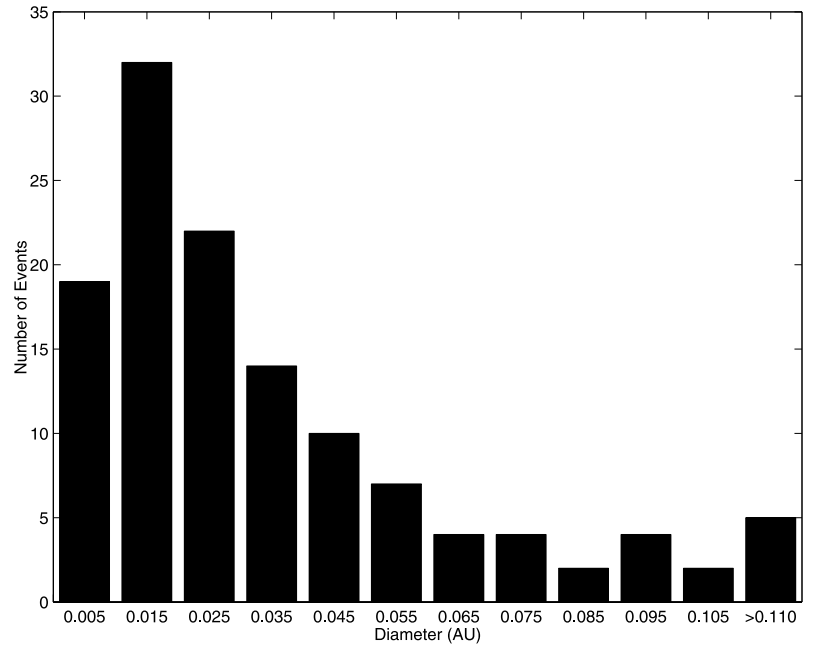

Figure 7. The distribution for diameters of SMCs.

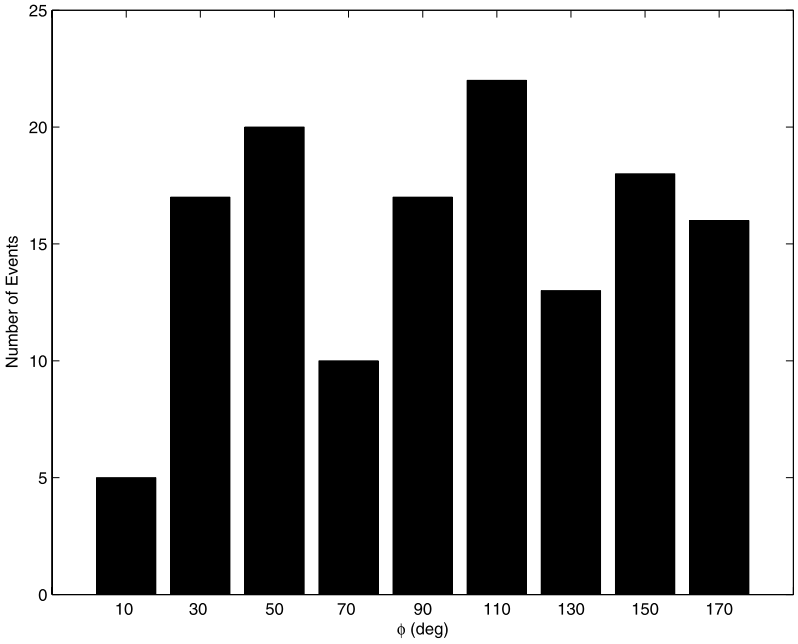

Figure 8. The distribution for the longitudes of the axes of SMCs.

all cases falling in the first two quadrants. From Figure 8 we can find that the distributions of axial longitude are scattered and have no obvious tropism, which is in agreement with the statistical results of MCs shown in Figure 7 of the work of *Lepping and Berdichevsky* [2000] and also in agreement with Figure 4 of the work of *Marubashi* [2000]. However, the latitudinal distribution of the axial orientations has a directional tendency that, as can be seen in Figure 9, the cases with small latitudinal inclinations dominate the distribution. From Figure 9, we can find that the latitudes were predominantly within ±50°, and the distribution is Gaussian like. *Lepping and Berdichevsky* [2000] showed the similar results for MCs. Therefore we demonstrate that the axial orientations of the SMCs and MCs have a similar character.

4. Conclusions and Summary

[16] In the past more than two decades, there are a number of investigations for large scale flux ropes (viz. MCs; see section 1). However, there are only a few of studies in the literature for SMCs. Previously, *Moldwin et al.* [2000] reported several events. In this paper, we undertake a comprehensive study of SMC, and we also compared

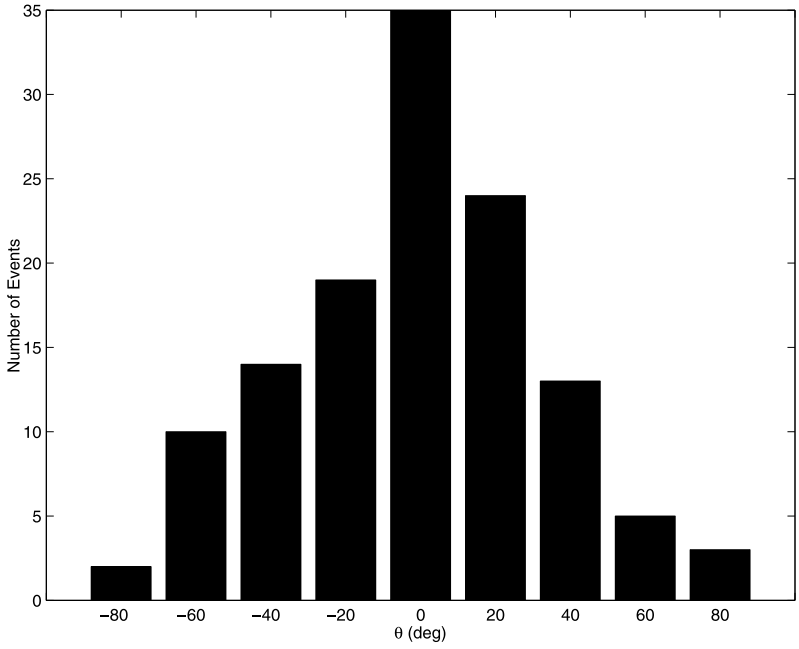

Figure 9. The distribution for the latitudes of the axes of SMCs.

their statistical properties with that of MCs. Using the interplanetary plasma and magnetic field data measured by Wind, we have identified 125 SMCs near the Earth during 1995 to 2005. The results show that the number of SMCs is much larger than that of MCs. We fitted all the identified SMCs by use of constant alpha force-free field model and provided the corresponding fitting parameters. The statistical properties were obtained and compared with that of MCs, the results appear that they have similar (or relative) characters as:

[17] 1. Both SMCs and MCs have the unusually low occurrence rate in 1999, and their trends of occurrence rate are approximately consistent.

[18] 2. Average speeds of the individual SMCs varied from 289 to 790 km/s with a mean value of 420 ± 86 km/s. Like MCs, most SMCs were found to have a propagation speed similar to that of typically slow (300–500 km/s) solar wind; only a few events had speeds comparable to the typically high (700–800 km/s) speed solar wind.

[19] 3. Average magnetic field strength of the individual SMC varies from 2.2 to 21.8 nT with a mean value of 8.1 ± 0.3 nT, which is less than the average magnetic field strengths of MCs, however, the mean value is larger than that of the background solar wind.

[20] 4. For both the SMCs and MCs, the distributions of axial longitude are scattered and have no obvious tropism, however, the distributions of axial latitude have a prominent tropism and were predominantly within ±50°.

[21] These similar characters may imply both the MCs and SMCs originate from solar eruptions, like MCs are interplanetary manifestations of ordinary CMEs, the SMCs are the interplanetary manifestations of small coronal mass ejections produced in small solar eruptions. In fact, in a recent work, *Mandrini et al.* [2005a, 2005b] have provided some direct evidence for a small eruption observed on the solar disc center linking to a SMC (no. 50 in Table 1). This evidence includes the timing, the same magnetic field direction and magnetic helicity sign in the coronal loop and in the rope, and comparable magnetic flux measured in the dimming regions and in the rope. In particular, the pre- to postevent change of magnetic helicity in the solar corona (the coronal magnetic helicity was estimated using *Berger*'s [1985] model) is found to be comparable to the helicity content of the rope. It should be noticed that the SMCs have two obvious differences from MCs although they have similar (or relative) characters. One is the difference in proton density behavior. The proton density in MCs is consistently lower than the ambient solar wind but the temperature changes vary little across SMCs. The other one is the lack of apparent expansion of the SMCs, but MCs usually are still expanding at 1 AU. One possible explanation is that the magnetic field is weaker inside these small-scale structures, on the other hand, both density and temperature change very little across SMCs. Therefore SMCs are close to pressure balance with the surrounding solar wind, SMCs have no apparent expansion signature. Finally, it is necessary to point out that the present work cannot absolutely exclude the possibility of the interplanetary origin of SMCs, although this study interprets the "different but similar" characteristics of SMC and MC as suggesting a common source mechanism, there are differences that aren't readily explained. Perhaps, SMCs have two formation mechanisms: some are small-scale CME and others have an interplanetary origin. However, currently it is difficult to distinguish between the two formation mechanisms and further observations are needed.

[22] **Acknowledgments.** This work was supported by National Nature Science Foundation of China (NSFC) under grant nos. 40804034, 10425312, 10603014, and 40574065 and by a project supported by the Specialized Research Fund for State Key Laboratories, and it is also supported by National Science Council (NSC) (Taiwan) under grants NSC 97-2111-M-008-012-MY3 and NSC 97-2811-M-008-039 to National Central University. The authors thank NASA/GSFC for the use of the key parameters from Wind obtained via the CDA Web page.

[23] Zuyin Pu thanks the reviewers for their assistance in evaluating this paper.

References

Berger, M. A. (1985), Structure and stability of constant-alpha force-free fields, *Astrophys. J. Suppl. Ser.*, *59*, 433.

Bothmer, V., and R. Schwenn (1996), Signatures of fast CMEs in interplanetary space, *Adv. Space Sci.*, *17*, 319–322.

Bothmer, V., and R. Schwenn (1998), The structure and origin of magnetic clouds in the solar wind, *Ann. Geophys.*, *16*, 1–24.

Burlaga, L. F. (1988), Magnetic clouds and force-free fields with constant alpha, *J. Geophys. Res.*, *93*, 7217–7224.

Burlaga, L. F. (1991), Magnetic clouds, in *Physics of the Inner Heliosphere II: Particles, Waves, and Turbulence*, edited by R. Schwenn and E. Marsch, pp. 1–19, Springer, New York.

Burlaga, L. F. (1995), Interplanetary magnetohydrodynamics, Oxford Univ. Press, New York.

Burlaga, L. F., and K. W. Behannon (1982), Magnetic clouds: Voyager observations between 2 and 4 AU, *Sol. Phys.*, *81*, 181.

Burlaga, L. F., E. Sittler, F. Mariani, and R. Schwenn (1981), Magnetic loop behind an interplanetary shock: Voyager, Helios, and IMP 8 observations, *J. Geophys. Res.*, *86*, 6673–6684.

Burlaga, L. F., R. Lepping, and J. A. Jones (1990), Global configuration of a magnetic cloud, in *Physics of Magnetic Flux Ropes*, *Geophys. Monogr. Ser.*, vol. 58, edited by C. T. Russell, E. R. Priest, and L. C. Lee, pp. 343–364, AGU, Washington, D. C.

Cane, H. V., and I. G. Richardson (2003), Interplanetary coronal mass ejections in the near-Earth solar wind during 1996–2002, *J. Geophys. Res.*, *108*(A4), 1156, doi:10.1029/2002JA009817.

Cane, H. V., I. G. Richardson, and O. C. St. Cyr (2000), Coronal mass ejections, interplanetary ejecta and geomagnetic storms, *Geophys. Res. Lett.*, *27*, 3591–3594.

Echer, E., and W. D. Gonzalez (2004), Geoeffectiveness of interplanetary shocks, magnetic clouds, sector boundary crossings and their combined occurrence, *Geophys. Res. Lett.*, *31*, L09808, doi:10.1029/2003GL019199.

Farrugia, C. J., V. A. Osherovich, and L. F. Burlaga (1995), Magnetic flux rope versus the spheromak as models for interplanetary magnetic clouds, *J. Geophys. Res.*, *100*, 12,293–12,306.

Feng, H. Q., D. J. Wu, and J. K. Chao (2006), Identification of configuration and boundaries of interplanetary magnetic clouds, *J. Geophys. Res.*, *111*, A07S90, doi:10.1029/2005JA011509.

Feng, H. Q., D. J. Wu, and J. K. Chao (2007), Size and energy distributions of interplanetary magnetic flux ropes, *J. Geophys. Res.*, *112*, A02102, doi:10.1029/2006JA011962.

Goldstein, H. (1983), On the field configuration in magnetic clouds, in *Solar Wind Five*, edited by M. Neugebauer, *NASA Conf. Publ.*, *2280*, 731–733.

Gopalswamy, N. (2006), Properties of interplanetary coronal mass ejections, *Space Sci. Rev.*, *124*, 145–168.

Gopalswamy, N., A. Lara, S. Yashiro, S. Nunes, and R. A. Howard (2003), Coronal mass ejection activity during solar cycle 23, in *Solar Variability as an Input to the Earth's Environment: International Solar Cycle Studies (ICS) Symposium, 23–28 June 2003, Tatranska Lomnica, Slovak Republic*, edited by A. Wilson, *Eur. Space Agency Spec. Publ.*, *ESA SP-535*, 403–414.

Hidalgo, M. A. (2003), A study of the expansion and distortion of the cross section of magnetic clouds in the interplanetary medium, *J. Geophys. Res.*, *108*(A8), 1320, doi:10.1029/2002JA009818.

Hidalgo, M. A., and C. Cid (2002), A non-force-free approach to the topology of magnetic clouds in solar wind, *J. Geophys. Res.*, *107*(A1), 1002, doi:10.1029/2001JA900100.

Hu, Q., and B. U. O. Sonnerup (2002), Reconstruction of magnetic clouds in the solar wind: Orientations and configurations, *J. Geophys. Res.*, *107*(A7), 1142, doi:10.1029/2001JA000293.

Hundhausen, A. J. (1998), The origin and propagation of coronal mass ejections, in *Proc. of the Sixth Int. Solar Wind Conf.*, edited by V. Pizzo, T. E. Holzler, and D. G. Sime, *Tech. Note NCAR/TN-306+Proc.*, pp. 181–214, Natl. Cent. for Atmos. Res., Boulder, Colo.

Kahler, S. (1988), Observations of coronal mass ejections near the Sun, *Solar Wind Six*, edited by V. J. Pizzo, T. E. Holzer, and D. G. Sime, *Tech. Note NCAR/TN-306+Proc. 181*, pp. 215, Natl. Cent. for Atmos. Res., Boulder, Colo.

Leamon, R. J., R. C. Canfield, S. L. Jones, K. Lambkin, B. J. Lundberg, and A. A. Pevtsov (2004), Helicity of magnetic clouds and their associated active regions, *J. Geophys. Res.*, *109*, A05106, doi:10.1029/2003JA010324.

Lepping, R. P., and D. Berdichevsky (2000), Interplanetary magnetic clouds: Sources, properties, modeling, and geomagnetic relationship, *Recent Res. Dev. Geophys.*, *3*, 77–96.

Lepping, R. P., L. F. Burlaga, and J. A. Jones (1990), Magnetic field structure of interplanetary magnetic clouds at 1 AU, *J. Geophys. Res.*, *95*, 11,957–11,965.

Lepping, R. P., D. B. Berdichevsky, and T. J. Ferguson (2003), Estimated errors in magnetic cloud model fit parameters with force-free cylindrically symmetric assumptions, *J. Geophys. Res.*, *108*(A10), 1356, doi:10.1029/2002JA009657.

Lundquist, S. (1950), Magnetohydrostatic fields, *Ark. Fys.*, *2*, 361–365.

Mandrini, C. H., et al. (2005a), Interplanetary flux rope ejected from a X-ray bright point: The smallest magnetic cloud source-region ever observed, *Astron. Astrophys.*, *434*, 725–740.

Mandrini, C. H., et al. (2005b), The smallest source region of an interplanetary magnetic cloud: A mini-sigmoid, *Adv. Space Sci.*, *36*, 1579–1586.

Mariani, F. F. B., and F. M. Neubauer (1990), The Interplanetary magnetic field, *Physics of the Inner Heliosphere I: Large-Scale Phenomena*, edited by R. Schwenn and E. Marsch, p. 183, Springer, New York.

Marsh, E. (1991), MHD turbulence in the solar wind, in *Physics of the Inner Heliosphere II: Particles, Waves, and Turbulence*, edited by R. Schwenn and E. Marsch, pp. 159, Springer, New York.

Marubashi, K. (2000), Physics of interplanetary magnetic flux ropes toward prediction of geomagnetic storms, *Adv. Space Res.*, *26*, 55–66.

Moldwin, M. B., S. Ford, R. Lepping, J. Slavin, and A. Szabo (2000), Small-scale magnetic flux ropes in the solar wind, *Geophys. Res. Lett.*, *27*, 57–60.

Ogilvie, K. W., D. J. Chornay, and R. J. Fritzenreiter (1995), SWE, A comprehensive plasma instrument for the Wind Spacecraft, *Space Sci. Rev.*, *71*, 55–77.

Riley, P., et al. (2004), Fitting flux ropes to a global MHD solution: A comparison of techniques, *J. Atmos. Sol. Terr. Phys.*, *66*, 1321–1331.

Smith, C. W., and J. L. Phillips (1997), The role of coronal mass ejections and interplanetary shocks in interplanetary magnetic field statistics and solar magnetic flux ejection, *J. Geophys. Res.*, *102*, 249–261.

Wei, F., R. Liu, Q. Fan, and X. Feng (2003), Identification of the magnetic cloud boundary layers, *J. Geophys. Res.*, *108*(A6), 1263, doi:10.1029/2002JA009511.

Wu, C.-C., and R. P. Lepping (2002), Effects of magnetic clouds on the occurrence of geomagnetic storms: The first 4 years of Wind, *J. Geophys. Res.*, *107*(A10), 1314, doi:10.1029/2001JA000161.

Wu, C.-C., and R. P. Lepping (2007), Comparison of the characteristics of magnetic clouds and magnetic cloud-like structures for the events of 1995–2003, *Sol. Phys.*, *242*, 159–165.

Wu, D. J., J. K. Chao, and R. P. Lepping (2000), Interaction between an interplanetary magnetic cloud and the Earth's magnetosphere: Motions of the bow shock, *J. Geophys. Res.*, *105*, 12,627–12,638.

Wu, C.-C., R. P. Lepping, and N. Gopalswamy (2006), Relationships among magnetic clouds, CMEs and geomagnetic storms, *Sol. Phys.*, *239*, 449–460.

Zhang, J.-C., M. W. Liemohn, J. U. Kozyra, B. J. Lynch, and T. H. Zurbuchen (2004), A statistical study of the geoeffectiveness of magnetic clouds during high solar activity years, *J. Geophys. Res.*, *109*, A09101, doi:10.1029/2004JA010410.

J. K. Chao, L. C. Lee, C. C. Lin, and L. H. Lyu, Institute of Space Science, National Central University, 300 Jhongda Rd., Jhongli, Taiwan. (jkchao@jupiter.ss.ncu.edu.tw; leelou@plasma.phys.ncku.edu.tw; dannylin@jupiter.ss.ncu.edu.tw; lyu@jupiter.ss.ncu.edu.tw)

H. Q. Feng, College of Physics and Electronic Information, Luoyang Normal University, 71 Longmen Road, Luoyang, Henan 471002, China. (fenghq9921@163.com)

D. J. Wu, Purple Mountain Observatory, Chinese Academy of Sciences, 2 West Beijing Rd., Nanjing, China.